



Basic Neuroscience

Use of vivo-morpholinos for control of protein expression in the adult rat brain

Kathryn J. Reissner*, Gregory C. Sartor, Elena M. Vazey, Thomas E. Dunn, Gary Aston-Jones, Peter W. Kalivas

Department of Neurosciences, Medical University of South Carolina, Charleston, SC 29425, United States

ARTICLE INFO

Article history:

Received 31 July 2011

Received in revised form 10 October 2011

Accepted 11 October 2011

Keywords:

Vivo-morpholino

GLT-1

xCT

Orexin

Antisense

Hypocretin

Nucleus accumbens

Lateral hypothalamus

ABSTRACT

Vivo-morpholinos are commercially available morpholino oligomers with a terminal octa-guanidinium dendrimer for enhanced cell-permeability. Existing evidence from systemically delivered vivo-morpholinos indicate that genetic suppression can last from days to weeks without evidence of cellular toxicity. However, intravenously delivered vivo-morpholinos are ineffective at protein suppression in the brain, and no evidence is available regarding whether intracranially delivered vivo-morpholinos effectively reduce target protein levels, or do so without inducing neurotoxicity. Here we report examples in which *in vivo* microinjection of antisense vivo-morpholinos directed against three different targets (xCT, GLT1, orexin) in two different brain regions resulted in significant suppression of protein expression without neurotoxicity. Expression was significantly suppressed at six to seven days post-administration, but returned to baseline levels within fourteen days. These results indicate that direct intracranial administration of vivo-morpholinos provides an effective means by which to suppress protein expression in the brain for one to two weeks.

© 2011 Elsevier B.V. All rights reserved.

1. Introduction

Effective methods for temporally controlled genetic suppression in the developed brain are critical for investigating the contribution of specific gene products to adult nervous system function. Although current transgenic methods provide sophisticated tools in this regard, behavioral methods that are optimized for use in rat models are limited, in large part due to technical hurdles in generating transgenic rat models (Aitman et al., 2008; Tesson et al., 2005). Nonetheless, direct brain microinjection of pharmacological agents, antisense oligonucleotides, and RNAi allow complementary approaches to genetic suppression that are useful in rat models (Self, 2005). However, acute administration of RNAi typically leads to transient suppression, and extended suppression requires the use of continual administration by mini-pump, or delivery via a viral vector (Morris, 2008).

In parallel with the development of transgenic and oligonucleotide (DNA and RNA) based methods, morpholino oligomers have emerged as an alternative and promising approach. Morpholino antisense technologies are widely used in a number of systems including rodent embryos, *Xenopus*, zebrafish, sea urchin and others (Corey and Abrams, 2001; Heasman, 2002). A morpholino antisense approach offers comparable or superior suppression to DNA oligonucleotides and RNAi, but with enhanced

structural stability and without many of the described non-specific, off-target effects (Summerton, 2007). This is due in part to the six-membered morpholino backbone and non-ionic phosphorodiamidate linkage, which limits interactions with the extracellular matrix and renders oligomers resistant to nuclease degradation (Summerton, 2007). Morpholinos suppress protein expression by binding to mRNA with high affinity and thus block translation or splicing, depending on the sequence location at translation initiation start sites or intron/exon junctions (Li and Morcos, 2008; Moulton and Jiang, 2009; Moulton and Yan, 2008).

A recent derivative of morpholinos are vivo-morpholinos. Vivo-morpholinos are designed from the same structure as morpholinos described above, with an additional octa-guanidinium dendrimer conjugated at the terminal 3' end (Moulton and Jiang, 2009). The dendrimer (derived from Greek for "tree") is a branched molecule, generally symmetrical and overall spherical in shape. In this case, the dendrimer is formed by the presence of either octa-guanidinium groups. This terminal attachment allows for facilitated cell permeability, via chemistry similar to that employed by TAT and other related peptide membrane permeability domains (Wadia and Dowdy, 2005). While vivo-morpholinos are superior to non-conjugated morpholinos for achieving suppression following *i.v.* administration, brain tissue is not significantly accessed following systemic delivery (Li and Morcos, 2008; Morcos et al., 2008; Parra et al., 2011). A few examples of successful knockdown with non-conjugated morpholinos administered directly in the brain have been reported (Hiroi et al., 2011; Oh et al., 2006). However, evidence is not available

* Corresponding author. Tel.: +1 843 792 1838; fax: +1 843 792 4423.
E-mail address: reissner@musc.edu (K.J. Reissner).

on the efficacy or toxicity of *vivo*-morpholinos administered intracranially.

Here we demonstrate use of *vivo*-morpholinos for genetic suppression in the adult rat brain, using three separate targets: the high-affinity glutamate transporter GLT-1/EAAT2, the catalytic subunit of the cystine glutamate exchanger xCT, and orexin/hypocretin. Important roles for glutamate transport by GLT-1 and xCT have been described in addiction, affective disorders, and protection against neurotoxicity and ischemia (Albrecht et al., 2010; Reissner and Kalivas, 2010; Valentine and Sanacora, 2009). The orexins are implicated in mechanisms of sleep as well as in motivation to obtain both natural rewards and drugs of abuse (Aston-Jones et al., 2010; Berridge et al., 2010; Cason et al., 2010; Thompson and Borgland, 2011). Because these targets are all of interest in the mechanisms of reward learning, we wished to determine applicability of *vivo*-morpholinos for temporal and regional control of protein expression. These results indicate that *vivo*-morpholinos can be effectively used to suppress protein expression in the brain *in vivo*, in a region-specific manner for a period of days to weeks, thus providing a genetic tool for the use of nervous system function and behavioral analysis without the necessity of transgenic or viral-mediated strategies.

2. Materials and methods

2.1. Animal housing and procedures

Adult male Sprague-Dawley rats (300–350 g, Charles River) were used for all studies. Animals were individually housed on a 12-h reverse-light cycle and provided rat chow and water ad libitum. Animals were anesthetized with ketamine/xylazine (56.5 mg/kg; 8.7 mg/kg, *i.p.*) and placed in the stereotaxic apparatus.

For injections into nucleus accumbens core (NAc), cannulae (Plastics One, 26G) were surgically implanted bilaterally into NAc coordinates relative to Bregma +1.5 A/P, +1.7 M/L, –5.5 D/V (Paxinos and Watson, 2005). Following one week of recovery, microinjections (1.0 μ l, 0.5 μ l/min) were made using 33G microinjectors (PlasticsOne) 2 mm below the base of the cannula. Microinjectors were left in place to allow a one min diffusion time following microinjection of awake animals (GLT-1, xCT). A sham insertion of the microinjection needle was performed on the day prior to the first microinjection, following which microinjections were performed once per day for three days, unless described otherwise. Canula were cased with obturators to prevent clogging between microinjections.

For orexin morpholino injections, a midline scalp incision was made and a small hole was drilled through the skull above the lateral hypothalamus (LH). With the dura removed, a 28 gauge cannula connected to a Hamilton syringe (via polyethylene tubing) was lowered in the LH orexin cell field at A/P –2.8, M/L 1.7, DV –8.8 from skull surface. In this case following microinjections, microinjectors were left in place for 15 min.

2.2. Morpholinos

All *vivo*-morpholinos were purchased from Gene Tools, LLC. The antisense sequence used for GLT-1 is 5'-TGTTGGCACCTCGGTTGATGCCAT-3', and for xCT is 5'-TGGCCACAACCTGGCTTCTGACCAT-3'. For these genes, a reverse sequence control was used. Dilution of morpholinos was performed in sterile PBS (10 mM Na₂HPO₄, 2 mM KH₂PO₄, 137 mM NaCl, 2.7 mM KCl). Orexin *vivo*-morpholinos (150 nmol, 0.3 μ l) or *vivo*-morpholino standard control (0.3 μ l) were unilaterally injected into the LH in the PBS formulation provided by the manufacturer. The antisense sequence used for orexin is

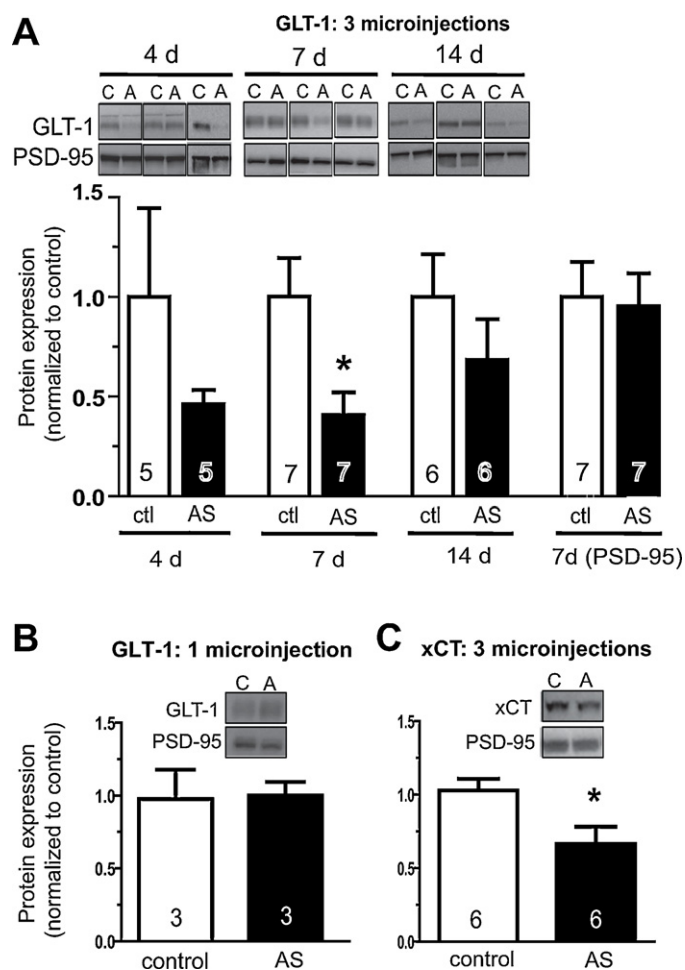


Fig. 1. Knockdown of GLT-1 and xCT in rat NAc with antisense *vivo*-morpholinos. Antisense (AS) or reverse control (ctl) sequence *vivo*-morpholinos against the indicated target were microinjected into contralateral hemispheres once per day for three days, and expression was assessed by Western blotting in a membrane subfraction at the indicated number of days following the last microinjection. Expression of xCT and GLT-1 was normalized to expression for PSD-95 loading control, and within animal comparisons were made between control and AS treatment for each animal. For representative blots, C, control; A, antisense. (A) Expression of GLT-1 is decreased at 4 days post-injection, and is significantly suppressed seven days post-microinjection. Levels of GLT-1 are not significantly different between AS and control treatments at fourteen days post-microinjection. Two-way ANOVA revealed a significant effect of treatment, $F(1,34) = 7.027, p < 0.05$. Because within animal comparison was used for each animal, a paired *t*-test was used for direct comparison at each time point. (B) One microinjection of GLT-1 AS *vivo*-morpholinos is insufficient to suppress expression seven days later. (C) Three microinjections of xCT AS *vivo*-morpholinos leads to significant suppression of expression seven days later, as compared by Western blot to reverse control-treated hemisphere.

5'-GTATCTTCGGTGCAGTGGTCCAAAT-3' and for the standard control is 5'-CCTCTTACCTCATTACAATTATA-3'.

2.3. Western blotting

For experiments in NAc (using morpholinos for GLT-1 and xCT), Western blots were used to assess changes in protein expression in a crude membrane subfraction as described (Knackstedt et al., 2010). Animals were rapidly decapitated, and NAc tissue surrounding the microinjection site was dissected. Individual hemispheres were separately homogenized in ice-cold 0.2 ml buffer containing Na Heps and sucrose, pH 7.4. All buffers were supplemented with 1:100 protease and phosphatase inhibitor cocktails (Thermo Scientific). Homogenates were centrifuged at 1000 \times g for 10 min at 4°C, and the pellet was homogenized with an additional 0.2 ml

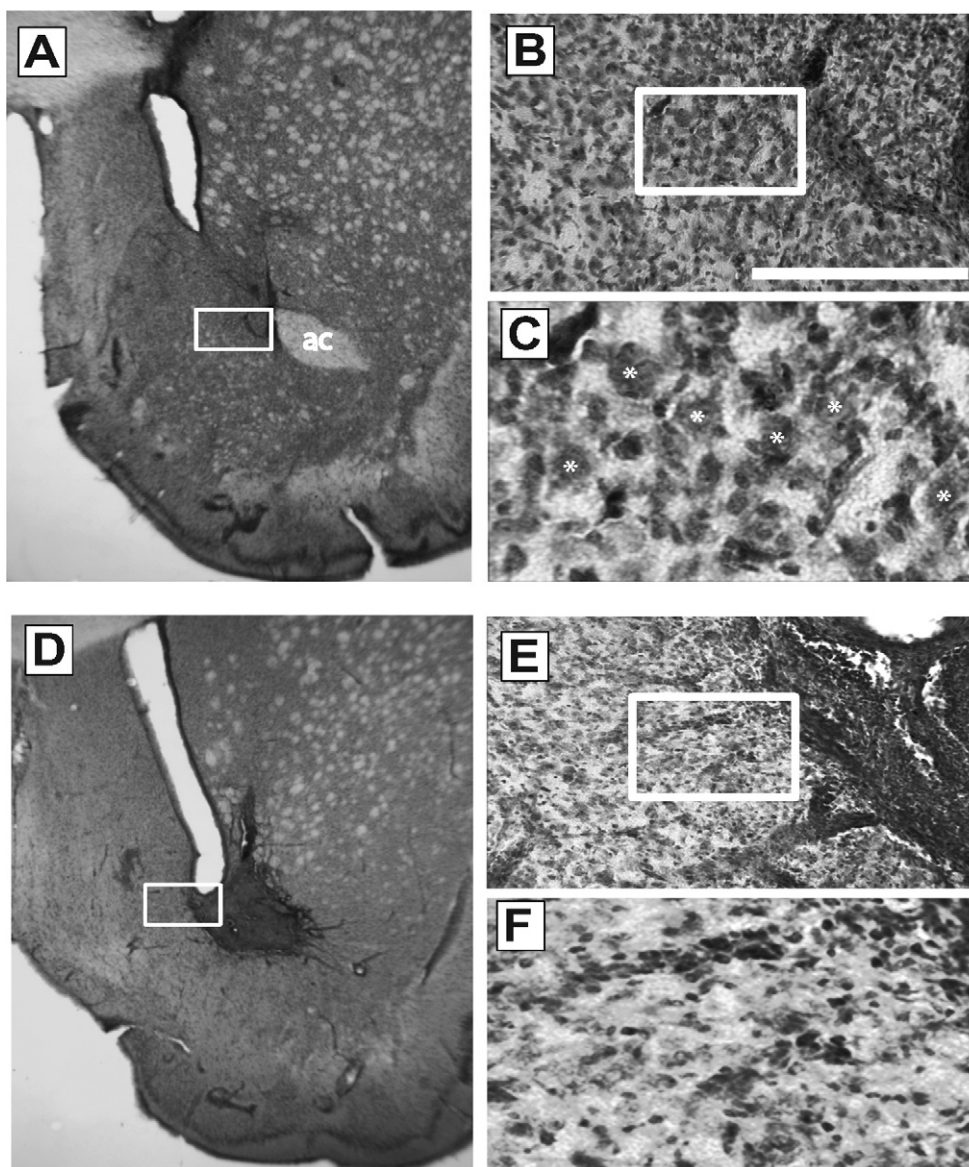


Fig. 2. Assessment of *vivo*-morpholinos toxicity by Nissl stain. All images show representative slices from animals microinjected with control *vivo*-morpholino for GLT-1 at either the low (A–C, 30 nmol) or high (D–F, 1500 nmol) dose. (A) Staining of NAc microinjected with low dose. (D) Staining of NAc microinjected with the high dose. Note the lack of staining of the anterior commissure as seen in panel A (region under “ac”), primary due to the induction of overt neurotoxic damage. (B, C and E, F); 20× and 60× magnification of regions boxed in (A) and (D). Comparison at 60× magnification in (C) and (F) indicates neurotoxicity as evidenced by smaller, more punctuate staining of cells. Stars in panel C indicate representative healthy medium spiny neurons. Scale bar, 100 μm at 20× magnification; ac, anterior commissure.

homogenization buffer, and centrifuged again. Supernatants were pooled and centrifuged at $12,000 \times g$ for 20 min. The resultant pellet was resuspended in 30 μl RIPA buffer (Thermo Scientific) supplemented with 1.0% SDS as well as protease and phosphatase inhibitors. A final centrifugation step at $10,000 \times g$ for 5 min was performed to remove insoluble material. Protein concentration was determined using the BCA method (Thermo Scientific) and equal microgram quantities were loaded per lane. Antibodies used were as follows: GLT-1, abcam ab41621 at 1:400, xCT custom antibody at 1:100 (Shih et al., 2006), PSD-95, Cell Signaling #2507 at 1:1000. Western blotting was performed onto nitrocellulose membranes using standard techniques, as described previously (Toda et al., 2006). Expression of GLT-1 and xCT was normalized to PSD-95.

2.4. Histology and immunohistochemistry

For Nissl staining, animals were deeply anesthetized with pentobarbital and perfused with saline. Brains were fixed in 4%

formaldehyde, and 100 μm sections taken for histological analysis. Sections were Nissl stained using Cresyl Violet.

For experiments in LH (orexin morpholino), changes in protein expression were assessed using immunohistochemistry. Rats were deeply anesthetized with ketamine/xylazine (100 mg/kg:20 mg/kg, i.p.) before being perfused transcardially with cold 0.9% saline followed by 4% paraformaldehyde. For orexin and MCH staining, brains were stored in 4% paraformaldehyde overnight and then transferred to 20% sucrose for at least 48 h. Brains were then flash frozen in dry ice and cut in 40 μm-thick tissue sections. LH sections were processed for the visualization of melanin-concentrating hormone (MCH) and orexin. MCH was visualized by incubating the section in rabbit anti-MCH (Phoenix Pharm, 1:2500) overnight; biotinylated goat anti-rabbit secondary antibody (Jackson, 1:500) and avidin–biotin complex (ABC 1:500, Vector labs) for 1.5 h. Detection of MCH was performed with 3,3'-diaminobenzidine (DAB, Sigma) with nickel ammonium sulfate, producing a dark purple reaction product in the cytoplasm. Subsequently, orexin was visualized by

incubating the same tissue sections in goat anti-orexin A (Santa Cruz, 1:1000) overnight, and then biotinylated donkey anti-goat secondary (Jackson, 1:500), followed by ABC (1:500). Finally, sections were incubated in DAB to yield a brown reaction product in the cytoplasm.

For NeuN staining, slices were dehydrated in 50% ethanol for 30 min, then washed three times for 10 min each in PBS. Blocking was performed for 1 h at room temperature in PBS containing 10% fetal calf serum (FCS) and 2% triton X-100. Primary antibody against NeuN (Millipore #MAB377, 1:500) was added in PBS containing 5% FCS at 4 °C overnight. Following three washes in PBS at 10 min each, slices were incubated in alexafluor 488 conjugated donkey anti-mouse IgG secondary (Invitrogen cat #A21202), then washed again. Slide-mounted slices were treated with Prolong gold (Invitrogen) and allowed to dry before imaging. Imaging was performed on a Leica DMXR microscope with Openlab software.

2.5. Statistical analysis

Statistical analysis was performed using Graphpad Prism. Data are presented as means with SEM about the mean. The effect of morpholinos over time was analyzed using two-way ANOVA, and within-animal comparisons were performed using a paired two-tailed *t*-test. * denotes $p < 0.05$. Cell counts (SEM) of orexin and MCH neurons in LH were averaged across four sections per animal.

3. Results

3.1. Three consecutive microinjections of vivo-morpholinos are sufficient to suppress either GLT-1 or xCT in NAc

Initial experiments were used to assess knockdown of glutamate transporter GLT-1. Three daily microinjections of GLT-1 AS morpholinos (10 μ M, 30 nmol total) were made contralaterally to the reverse control sequence, and protein levels were assessed in NAc separately in each hemisphere seven days later. Expression of xCT and GLT-1 was normalized to PSD-95 because PSD-95 is enriched in the membrane subfraction preparation, should be unaffected by either antisense sequence, and is of a molecular weight

distinct from xCT (37 kD) and GLT-1 (62 kD). This protocol resulted in statistically reduced levels of GLT-1 at seven days after the last microinjection (Fig. 1A, middle panel). A slight decrease was observed at four days, followed by significant suppression at seven days, and expression had returned to baseline at fourteen days following the third microinjection. No effect on expression of PSD-95 loading control was observed (Fig. 1A, last panel). In contrast, GLT-1 levels were not reduced seven days after one microinjection (10 μ M, 10 nmol) (Fig. 1B).

To determine if xCT could also be suppressed in a similar manner, protein levels were assessed seven days following three microinjections of antisense versus control reverse sequence. As with GLT-1, xCT protein levels were significantly suppressed by local microinjection of antisense vivo-morpholinos into NAc (Fig. 1C).

3.2. Low dose vivo-morpholino administration is not neurotoxic

Because use of vivo-morpholinos directly in brain has not yet been reported, it was important to determine whether this octa-guanidinium dendrimer-containing reagent might be neurotoxic. Membrane permeable TAT peptide conjugates used for a similar purpose carry toxicity at concentrations approaching 100 μ M (Jones et al., 2005). Moreover, vivo-morpholinos have been reported to produce evidence of mild toxicity when applied to renal explants in culture for 24 h at 20 μ M, although treatment with 10 μ M produced no evidence of toxicity (Hartwig et al., 2010). Specific to this study, any toxicity caused by suppression of GLT-1 was of additional concern as homozygous knockout mice for GLT-1 experience lethal seizures, and increased susceptibility to neuronal damage (Tanaka et al., 1997). Moreover, changes in expression of GLT-1 have been associated with neurodegenerative disease (Maragakis and Rothstein, 2004; Sheldon and Robinson, 2007).

General tissue health and cell morphology was first examined using Nissl staining (Fig. 2). Daily microinjections (30 or 1500 nmol total over 3 days) were performed with control sequence against GLT-1 in contralateral hemispheres. Typical scarring resulted from cannulae implantation and repeated penetration of the 33 gauge needle below the indwelling guide cannula (Fig. 2A–C). However,

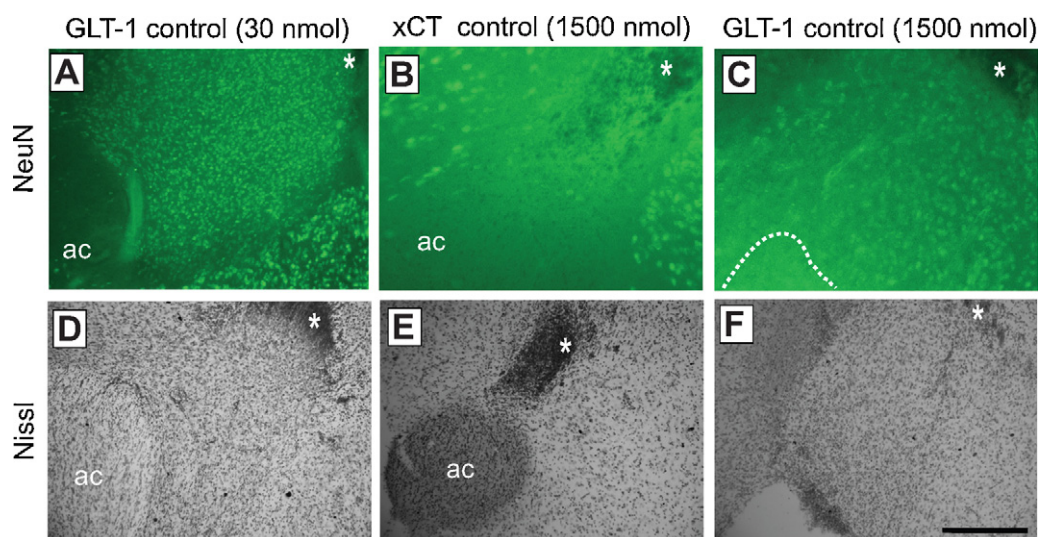


Fig. 3. Neurotoxicity observed following high dose vivo-morpholino treatment as assessed by NeuN. Top panel (A–C) shows NeuN immunostaining, while lower panel (D–F) shows Nissl staining of the same slice in the approximate same location. Note the tip of the microinjection site indicated by asterisk in (A–C). First column (A and D) shows staining following microinjection of low dose control vivo-morpholinos for GLT-1 (30 nmol). Middle column (B and E) and right column (C and F) show staining following microinjection of high dose control morpholinos for xCT and GLT-1 respectively at 10 \times magnification. In panel F, anterior commissure could not be visualized due to the presence of a hole in the tissue, likely caused by a neurotoxic lesion from the high dose morpholinos (indicated by dashed line in (C)). Scale bar, 100 μ m at 10 \times magnification. ac, anterior commissure.

microinjection of low dose (30 nmol) injection of *vivo*-morpholinos led to no discernable evidence of further damage (Fig. 2B–D). Upon high magnification, medium spiny neurons of typical triangular morphology were abundantly apparent adjacent to the microinjection site (Fig. 2C). Identical results were observed following microinjection of antisense for GLT-1, as well as control or antisense *vivo*-morpholinos for xCT (not shown). In contrast, microinjection of high dose (1500 nmol) control *vivo*-morpholinos resulted in evidence of apparent gross neuronal damage (Fig. 2d–F). High dose *vivo*-morpholino treatment resulted in neuronal loss and punctate Nissl staining (Fig. 2D and E) consistent with neurotoxic lesions and gliosis observed following chemical lesion of the striatum (Levivier et al., 1995; Zaczek et al., 1980).

In order to more fully assess any evidence for toxicity or cell loss induced by *vivo*-morpholinos, immunofluorescence for neuron-specific neuronal nuclei (NeuN) was performed (Mullen et al., 1992). One week following three consecutive microinjections of control *vivo*-morpholinos for GLT-1 or xCT at both low (30 nmol) and high (1500 nmol) dose, tissue was prepared for immunofluorescence. Microinjection of 30 nmol control GLT-1 resulted in abundant staining for neurons (Fig. 3A) which was indistinguishable from the same treatment with other *vivo*-morpholino sequences or PBS (data not shown). In contrast, high dose treatment of control morpholinos for either xCT or GLT-1 resulted in an obvious decrease in discrete neuronal staining (Fig. 3B and C). Following immunostaining, slices were then Nissl stained for direct comparison. In the condition of high dose treatment, similar overt neurotoxic lesions were observed as in Fig. 2, and in one case an obvious hole was observed in the NAC, in the location where the anterior commissure should be found (Fig. 3F).

3.3. *Vivo*-morpholinos suppress orexin

In a separate series of experiments, the capacity of *vivo*-morpholinos to suppress expression of orexin in the LH was assessed. In this case, knockdown of orexin was determined by immunohistochemical staining for orexin as well as melanin-concentrating hormone (MCH). MCH is expressed in interdigitated non-orexin neurons in the orexin cell field of the LH, and thus provides a good measure of the specificity of knockdown (Chen et al., 2006). One microinjection of morpholinos (0.3 μ l, 150 nmol) was sufficient to suppress orexin protein expression, but had no effect on MCH expression (Figs. 4 and 5). Similarly as observed for GLT-1, significant suppression of orexin was not observed 2–3 days post-microinjection of antisense, but was achieved by six days post-microinjection. Also, as seen with GLT-1 morpholinos, orexin expression levels returned to normal within fourteen days of microinjection (Fig. 4). However, microinjection of 1 μ l of morpholino (500 nmol) resulted in both orexin and MCH cell loss, indicating non-specific toxic effects at higher dosing (Fig. 5). Doses lower than 150 nmol were not tested for orexin. Finally, Nissl staining revealed no apparent toxicity within the orexin cell field at 6 days following the 150 nmol injection, but did indicate damage evidenced by lack of healthy neuron staining following the large 500 nmol injection (Fig. 5).

4. Discussion

Conventional non-transgenic methods for suppression of protein expression in adult rat brain include antisense oligonucleotides and RNAi. Although these techniques are effective, the time course of suppression is generally limited in the absence of continual infusion via osmotic minipump or viral vector. *Vivo*-morpholinos provide an alternative means by which expression may be controlled, utilizing different chemistry from canonical nucleic acid

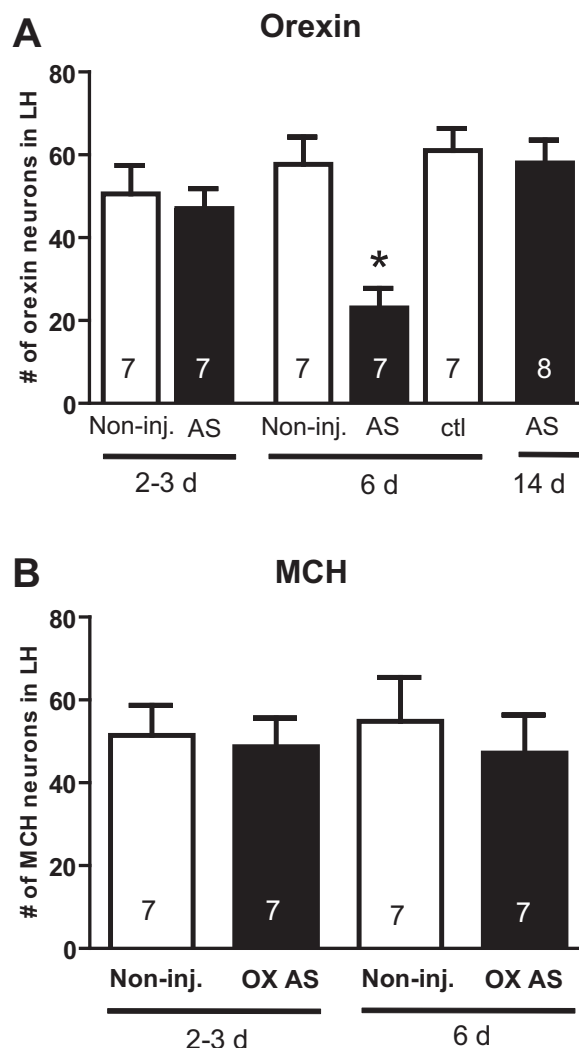


Fig. 4. Suppression of orexin expression in the LH by *vivo*-morpholinos. (A) Quantification of cell counts for orexin in the LH at different time points following control (ctl) or antisense (AS) *vivo*-morpholinos (150 nmol each). Non-inj. indicates cell counts in a non-injected control. One-way ANOVA ($F(5, 37) = 3.76, p < 0.01$). * indicates $p < 0.05$ by Tukey post hoc analysis. (B) Cell counts for MCH following treatment with orexin *vivo*-morpholinos. In both panels, N represents number of animals.

based technology. In this report, we provide evidence of knockdown of three different target proteins in two different brain structures. Comparison of the approach used for GLT-1/xCT versus orexin indicates that microinjection of *vivo*-morpholino may be made *in vivo* in anesthetized animals at the time of surgical cannula implantation (orexin) or following recovery in awake, moving animals (GLT-1/xCT). We further show that for these targets, the nontoxic effect dose is in the range of 30–150 nmol; however, toxicity is induced when injected amounts approach 500 nmol above.

The enduring stability and efficacy of *vivo*-morpholinos allows gene expression that can be temporally controlled, and enduring suppression can be achieved without continuous brain perfusion with a minipump. For example, treatment with naked (non-conjugated) morpholinos designed to remove a splicing mutation restores expression of muscle dystrophin as well as muscle function in *mdx* transgenic mice two to four weeks after morpholino treatment (Alter et al., 2006; Fletcher et al., 2007; Jearawiriyapaisarn et al., 2008; Sharp et al., 2011). Our findings with GLT-1 and orexin indicate that suppression of translation can be achieved for one to two weeks, thus allowing several days or more for analysis while

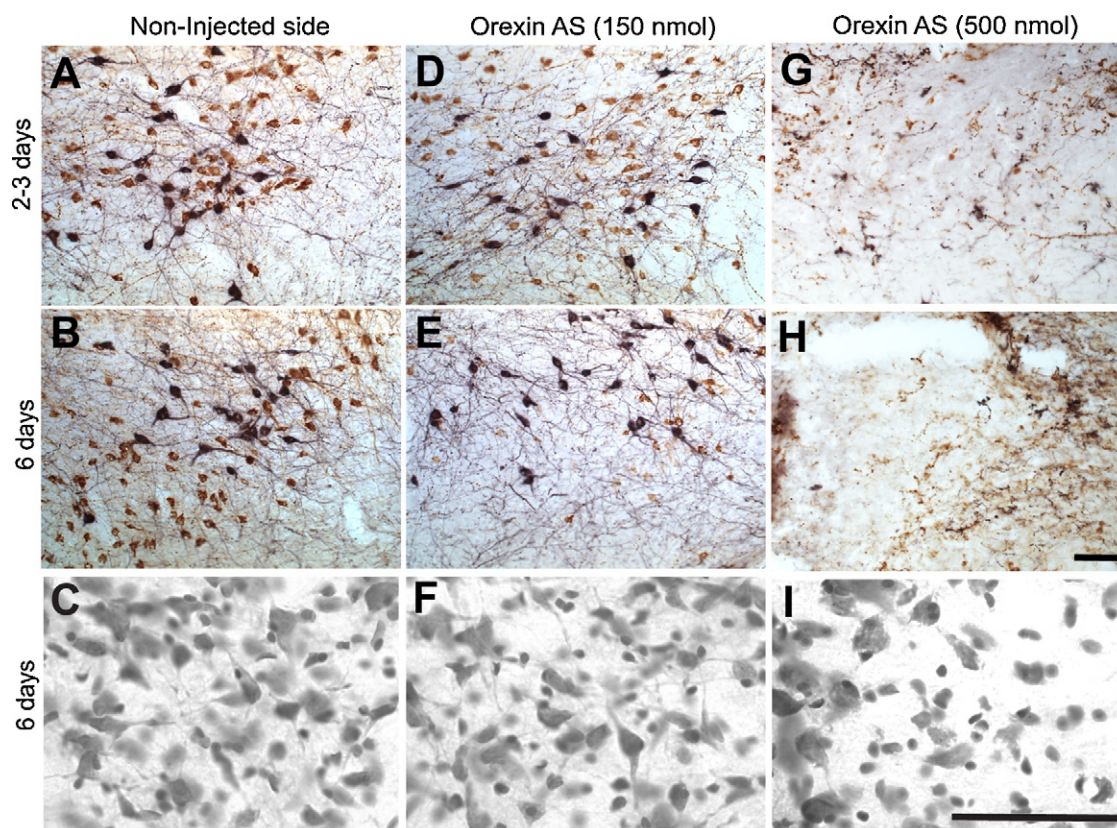


Fig. 5. Suppression of orexin in the LH visualized by immunostaining. Representative photomicrographs of double staining for orexin (brown) and MCH (black) in LH 2–3 or 6 days post-injection in the non-injected (control) sides (A–C) and orexin AS injected (D–F, low dose; G–I, high dose). Cresyl violet staining of adjacent tissue from the same sections shown in the middle row (B, E, and H) are shown below in panels C, F, and I. The number of orexin, but not MCH, expressing neurons was reduced 6 days after orexin AS injection. No reduction of orexin or MCH was observed 2–3 days after orexin AS injection. Apparent toxicity was observed following high dose (500 nm) treatment (G–I) by both immunostaining and Nissl staining. All images were taken within 160 μm of the injection site. Scale bar, 45 μm in first two rows at 20 \times , 100 μm on bottom row of Nissl images at 60 \times .

protein targets are knocked down, and comparison with testing before and after morpholino treatment.

Finally, staining for cell bodies with Cresyl violet and NeuN immunofluorescence suggest no cell loss or neurotoxicity when used at 30–150 nmol. Modest tissue damage was observed, which is frequently observed following mechanical disruption by cannulation. Optimal conditions will likely need to be determined for each target protein, as in the case of any knockdown strategy. We find that effective knockdown without toxicity is observed in the range of 30–150 nmol; however, it is possible that for some targets, knockdown can be optimized by higher amounts without induction of toxicity observed at 500 nmol and above. Overall, these results indicate that *vivo*-morpholinos are ideally suited for behavioral studies involving intracranial protein knock-down in selected brain nuclei, and for permitting repeated measures to be made both during protein knock-down and after levels have been restored.

Acknowledgements

This work is supported by NIH grants DA026254 (KJR), DA007288 (GCS), DA06214 (GAJ), and DA015369/DA003906 (PWK). The authors thank members of the Kalivas lab for constructive comments on a previous version of the manuscript.

References

Aitman TJ, Critser JK, Cuppen E, Dominiczak A, Fernandez-Suarez XM, Flint J, et al. Progress and prospects in rat genetics: a community view. *Nat Genet* 2008;40:516–22.

- Albrecht P, Lewerenz J, Dittmer S, Noack R, Maher P, Methner A. Mechanisms of oxidative glutamate toxicity: the glutamate/cystine antiporter system xc⁻ as a neuroprotective drug target. *CNS Neurol Disord Drug Targets* 2010;9:373–82.
- Alter J, Lou F, Rabinowitz A, Yin H, Rosenfeld J, Wilton SD, et al. Systemic delivery of morpholino oligonucleotide restores dystrophin expression bodywide and improves dystrophic pathology. *Nat Med* 2006;12:175–7.
- Aston-Jones G, Smith RJ, Sartor GC, Moorman DE, Massi L, Tahsili-Fahadan P, et al. Lateral hypothalamic orexin/hypocretin neurons: a role in reward-seeking and addiction. *Brain Res* 2010;1314:74–90.
- Berridge KC, Ho CY, Richard JM, DiFeliceantonio AG. The tempted brain eats: pleasure and desire circuits in obesity and eating disorders. *Brain Res* 2010;1350:43–64.
- Cason AM, Smith RJ, Tahsili-Fahadan P, Moorman DE, Sartor GC, Aston-Jones G. Role of orexin/hypocretin in reward-seeking and addiction: implications for obesity. *Physiol Behav* 2010;100:419–28.
- Chen L, Thakkar MM, Winston S, Bolortuya Y, Basheer R, McCarley RW. REM sleep changes in rats induced by siRNA-mediated orexin knockdown. *Eur J Neurosci* 2006;24:2039–48.
- Corey DR, Abrams JM. Morpholino antisense oligonucleotides: tools for investigating vertebrate development. *Genome Biol* 2001;2: Reviews 1015.
- Fletcher S, Honeyman K, Fall AM, Harding PL, Johnsen RD, Steinhaus JP, et al. Morpholino oligomer-mediated exon skipping averts the onset of dystrophic pathology in the mdx mouse. *Mol Ther* 2007;15:1587–92.
- Hartwig S, Ho J, Pandey P, Macisaac K, Taglienti M, Xiang M, et al. Genomic characterization of Wilms' tumor suppressor 1 targets in nephron progenitor cells during kidney development. *Development* 2010;137:1189–203.
- Heasman J. Morpholino oligos: making sense of antisense? *Dev Biol* 2002;243:209–14.
- Hiroi R, McDevitt RA, Morcos PA, Clark MS, Neumaier JF. Overexpression or knockdown of rat tryptophan hydroxylase-2 has opposing effects on anxiety behavior in an estrogen-dependent manner. *Neuroscience* 2011;176:120–31.
- Jearawiriyapaisarn N, Moulton HM, Buckley B, Roberts J, Sazani P, Fucharoen S, et al. Sustained dystrophin expression induced by peptide-conjugated morpholino oligomers in the muscles of mdx mice. *Mol Ther* 2008;16:1624–9.
- Jones SW, Christison R, Bundell K, Voyce CJ, Brockbank SM, Newham P, et al. Characterisation of cell-penetrating peptide-mediated peptide delivery. *Br J Pharmacol* 2005;145:1093–102.
- Knackstedt LA, Melendez RI, Kalivas PW. Ceftriaxone restores glutamate homeostasis and prevents relapse to cocaine seeking. *Biol Psychiatry* 2010;67:81–4.

- Levivier M, Gash DM, Przedborski S. Time course of the neuroprotective effect of transplantation on quinolinic acid-induced lesions of the striatum. *Neuroscience* 1995;69:43–50.
- Li YF, Morcos PA. Design and synthesis of dendritic molecular transporter that achieves efficient in vivo delivery of morpholino antisense oligo. *Bioconjug Chem* 2008;19:1464–70.
- Maragakis NJ, Rothstein JD. Glutamate transporters: animal models to neurologic disease. *Neurobiol Dis* 2004;15:461–73.
- Morcos PA, Li Y, Jiang S. Vivo-morpholinos: a non-peptide transporter delivers Morpholinos into a wide array of mouse tissues. *Biotechniques* 2008;45:613–4, 616, 618 passim.
- Morris KV. RNA-mediated transcriptional gene silencing in human cells. *Curr Top Microbiol Immunol* 2008;320:211–24.
- Moulton JD, Jiang S. Gene knockdowns in adult animals: PPMOs and vivo-morpholinos. *Molecules* 2009;14:1304–23.
- Moulton JD, Yan YL. Using Morpholinos to control gene expression. *Curr Protoc Mol Biol* 2008;26 [chapter 26: Unit 26 8].
- Mullen RJ, Buck CR, Smith AM. NeuN, a neuronal specific nuclear protein in vertebrates. *Development* 1992;116:201–11.
- Oh IS, Shimizu H, Satoh T, Okada S, Adachi S, Inoue K, et al. Identification of nesfatin-1 as a satiety molecule in the hypothalamus. *Nature* 2006;443:709–12.
- Parra MK, Gee S, Mohandas N, Conboy JG. Efficient in vivo manipulation of alternative pre-mRNA splicing events using antisense morpholinos in mice. *J Biol Chem* 2011;286:6033–9.
- Paxinos G, Watson C. The rat brain in stereotaxic coordinates. 5th ed. Amsterdam: Elsevier Academic; 2005.
- Reissner KJ, Kalivas PW. Using glutamate homeostasis as a target for treating addictive disorders. *Behav Pharmacol* 2010;21:514–22.
- Self DW. Molecular and genetic approaches for behavioral analysis of protein function. *Biol Psychiatry* 2005;57:1479–84.
- Sharp PS, Bye-a-Jee H, Wells DJ. Physiological characterization of muscle strength with variable levels of dystrophin restoration in mdx mice following local antisense therapy. *Mol Ther* 2011;19:165–71.
- Sheldon AL, Robinson MB. The role of glutamate transporters in neurodegenerative diseases and potential opportunities for intervention. *Neurochem Int* 2007;51:333–55.
- Shih AY, Erb H, Sun X, Toda S, Kalivas PW, Murphy TH. Cystine/glutamate exchange modulates glutathione supply for neuroprotection from oxidative stress and cell proliferation. *J Neurosci* 2006;26:10514–23.
- Summerton JE. Morpholino, siRNA, and S-DNA compared: impact of structure and mechanism of action on off-target effects and sequence specificity. *Curr Top Med Chem* 2007;7:651–60.
- Tanaka K, Watase K, Manabe T, Yamada K, Watanabe M, Takahashi K, et al. Epilepsy and exacerbation of brain injury in mice lacking the glutamate transporter GLT-1. *Science* 1997;276:1699–702.
- Tesson L, Cozzi J, Menoret S, Remy S, Usal C, Fraichard A, et al. Transgenic modifications of the rat genome. *Transgenic Res* 2005;14:531–46.
- Thompson JL, Borgland SL. A role for hypocretin/orexin in motivation. *Behav Brain Res* 2011;217:446–53.
- Toda S, Shen HW, Peters J, Cagle S, Kalivas PW. Cocaine increases actin cycling: effects in the reinstatement model of drug seeking. *J Neurosci* 2006;26:1579–87.
- Valentine GW, Sanacora G. Targeting glial physiology and glutamate cycling in the treatment of depression. *Biochem Pharmacol* 2009;78:431–9.
- Wadia JS, Dowdy SF. Transmembrane delivery of protein and peptide drugs by TAT-mediated transduction in the treatment of cancer. *Adv Drug Deliv Rev* 2005;57:579–96.
- Zaczek R, Simonton S, Coyle JT. Local and distant neuronal degeneration following intrastriatal injection of kainic acid. *J Neuropathol Exp Neurol* 1980;39:245–64.